

Published in final edited form as:

Ann Neurol. 2008 October ; 64(4): 388–401. doi:10.1002/ana.21451.

A β AMYLOID & GLUCOSE METABOLISM IN THREE VARIANTS OF PRIMARY PROGRESSIVE APHASIA

G.D. Rabinovici, MD^{1,2,3,4}, W.J. Jagust, MD^{1,2,3,4}, A.J. Furst, PhD^{3,4}, J.M. Ogar, MS^{1,5}, C.A. Racine, PhD^{1,2}, E.C. Mormino, BS^{3,4}, J.P. O'Neil, PhD⁴, R.A. Lal, BS³, N.F. Dronkers, PhD^{5,6}, B.L. Miller, MD^{1,2}, and M.L. Gorno-Tempini, MDPhD^{1,2}

¹ Memory and Aging Center, University of California San Francisco, San Francisco, California

² Department of Neurology, University of California San Francisco, San Francisco, California

³ Helen Wills Neuroscience Institute, University of California Berkeley, Berkeley, CA

⁴ Lawrence Berkeley National Laboratory, Berkeley, CA

⁵ Center for Aphasia and Related Disorders, VA Northern California Health Care System, Martinez, CA

⁶ Department of Neurology, University of California Davis, Davis, CA

Abstract

OBJECTIVE—Alzheimer's disease (AD) is found at autopsy in up to one-third of patients with primary progressive aphasia (PPA), but clinical features that predict AD pathology in PPA are not well defined. We studied the relationships between language presentation, A β amyloidosis and glucose metabolism in three variants of PPA using [¹¹C]PIB and [¹⁸F]FDG-PET.

METHODS—Patients meeting PPA criteria (N=15) were classified as logopenic aphasia (LPA), progressive non-fluent aphasia (PNFA) or semantic dementia (SD) based on language testing. [¹¹C]PIB distribution volume ratios were calculated using Logan graphical analysis (cerebellar reference). [¹⁸F]FDG images were normalized to pons. Partial volume correction was applied.

RESULTS—Elevated cortical PIB (by visual inspection) was more common in LPA (4/4 patients) than in PNFA (1/6) and SD (1/5) (p<0.02). In all PIB-positive cases, PIB uptake was diffuse and indistinguishable from the pattern in matched AD patients (N=10). FDG patterns were focal and varied by PPA subtype, with left temporoparietal hypometabolism in LPA, left frontal hypometabolism in PNFA, and left anterior temporal hypometabolism in SD. FDG patterns in PIB-positive PNFA and SD were similar to PIB-negative cases. Language regions showed asymmetric left hypometabolism in PPA (p<0.005) but not in AD.

INTERPRETATION—LPA is associated with A β amyloidosis, suggesting that sub-classification of PPA based on language features can help predict the likelihood of underlying AD pathology. Language phenotype in PPA is closely related to metabolic changes that are focal and anatomically distinct between subtypes, but not to amyloid deposition patterns that are diffuse and similar to AD.

Corresponding Author: Gil D. Rabinovici, MD, UCSF Memory & Aging Center, 350 Parnassus Ave., Suite 706, San Francisco, CA 94143, Tel.: (415) 514-9320, Fax: (415) 476-4800, Email: grabinovici@memory.ucsf.edu.

Disclosures: Dr. Jagust has received consulting fees from GE Healthcare, which holds a license agreement with the University of Pittsburgh based on the PIB compound described in this manuscript. The other authors do not report potential conflicts of interest.

Introduction

Primary progressive aphasia (PPA) is a clinical syndrome characterized by progressive loss of language function (with relative sparing of other cognitive domains) in the setting of focal degeneration of the dominant-hemisphere language network.^{1–3} The pathologic causes of PPA are heterogeneous and include tau-positive and TDP-43-positive variants of frontotemporal lobar degeneration (FTLD), corticobasal degeneration (CBD) and progressive supranuclear palsy (PSP).^{4–8} A significant minority of patients with PPA, estimated at 20% – 37% in recent pathologic series, are found to have Alzheimer’s disease (AD) on autopsy.^{4, 5, 8, 9} Identifying PPA patients with underlying AD during life is increasingly important, as they may be candidates for emerging therapies directed against beta-amyloid (A β).^{10, 11} However, clinical features that reliably discriminate between AD and non-AD causes of PPA are not yet well defined.

Clinical presentations of PPA can be classified into distinct variants based on the language phenotype.^{2, 12} These variants are associated with signature patterns of gray matter atrophy and glucose hypometabolism within the language network, and recent evidence suggests they are associated with differing underlying histopathologies.^{5, 9} The two most extensively studied PPA variants are progressive non-fluent aphasia (PNFA) and semantic dementia (SD).¹³ PNFA is characterized by effortful speech output, agrammatism, and apraxia of speech, with relative sparing of single word comprehension,^{12–15} while SD is distinguished by loss of word and object meaning, with fluent, grammatically correct speech.^{12, 14, 16} Anatomically, patients with PNFA demonstrate atrophy and hypometabolism in left inferior frontal gyrus and anterior insula,^{12, 17} while patients with SD show left anterior temporal lesions.^{12, 18, 19} At autopsy, PNFA is usually associated with the non-AD tau-inclusion disorders Pick’s disease, CBD and PSP,^{4, 5, 7, 20} while SD is more frequently linked to FTLD pathology with tau-negative, ubiquitin-and TDP-43-positive inclusions.^{5, 6, 21, 22}

A third PPA variant, logopenic aphasia (LPA), is characterized by slow speech output with word-finding difficulty and deficits in sentence repetition.^{12, 23–25} LPA patients may seem non-fluent due to their slow, hesitant speech, but they do not show agrammatism or motor speech deficits and are thus considered “fluent” in the classic aphasia nosology. Yet, LPA differs from the fluent aphasia of SD because of the relative sparing of single word comprehension and semantic memory.¹² LPA also differs anatomically from the other PPA variants, with patients showing maximal atrophy in the left temporoparietal junction.¹² This posterior pattern of atrophy, similar to the pattern reported in AD,²⁶ as well as the high frequency of the apolipoprotein E4 genotype in patients with LPA,¹² has led our group to hypothesize that LPA may be associated with underlying AD pathology.¹² This hypothesis was strengthened by recent retrospective observations that temporoparietal hypometabolism and atrophy were characteristic of PPA patients who were found to have AD at autopsy, and by two recent clinicopathological series that found AD pathology in ten of fourteen patients whose language deficits were retrospectively classified as LPA-like.^{27–29}

In this prospective study we sought to investigate the association between clinical features, patterns of glucose metabolism and AD pathology in PPA using the novel PET ligand [¹¹C]-labeled Pittsburgh compound-B ([¹¹C]PIB).³⁰ PIB binds specifically to fibrillar A β amyloid,^{30, 31} and PIB-PET signal measured *in vivo* correlates strongly with *in vitro* measures of fibrillar A β at autopsy.^{31, 32} PIB-PET can be useful in distinguishing between AD and non-AD causes of dementia,^{33, 34} and may be helpful in distinguishing between AD and other pathological causes of PPA that do not involve A β aggregation. We hypothesized that elevated cortical PIB indicative of A β amyloidosis would be common in patients with LPA, but uncommon in patients with PNFA and SD. Furthermore, we sought to combine molecular imaging with PIB with functional imaging with [¹⁸F]-labeled fluorodeoxyglucose ([¹⁸F]FDG)

in order to investigate the relationships between language phenotype, glucose metabolism, and the distribution of A β amyloid in PPA.

Methods

Subject Selection and Characterization

Patients were recruited from a PPA research cohort followed at the University of California San Francisco Memory and Aging Center (UCSF-MAC). All patients underwent a history and physical examination by a neurologist, a structured caregiver interview by a nurse, and a battery of neuropsychological tests.³⁵ Patients were eligible for the study if they met research criteria for PPA.² Specifically, all major limitations in activities of daily living were attributed to language impairment for at least two years from estimated symptom onset, and all patients had a language-predominant syndrome at the time of enrollment.² Patients with a history of a pre-existing speech or language disorder were excluded.

All patients meeting PPA criteria underwent a previously-described battery of speech and language tests in order to determine PPA subtype.¹² The battery includes portions of the Western Aphasia Battery (WAB),³⁶ Boston Diagnostic Aphasia Examination (BDAE),³⁷ Boston Naming Test (BNT),³⁸ Curtiss-Yamada Comprehensive Language Evaluation – Receptive Subtests (CYCLE-R),³⁹ the Pyramid and Palm Trees Test (PPT),⁴⁰ the Motor Speech Evaluation (MSE)⁴¹ and portions of the Psycholinguistic Assessments of Language Processing in Aphasia (PALPA).⁴² PPA subtypes were determined by consensus between two clinicians (MGT and JMO), with a third (NFD) recruited when needed. Initial subtype classification was based solely on language testing (including review of video segments from the testing sessions) and was blind to additional data (e.g. neurological examination, non-language neuropsychological testing or neuroimaging results) obtained during the patients' comprehensive clinical evaluations. Twelve of 15 patients included in the study had more than one evaluation at the MAC at the time of enrollment (mean follow up 1.9 years, range 0 – 4.7 years). Strict blinding of non-language clinical data could not be maintained for all of these patients. However, there were no instances in which subtype assignment changed with longitudinal follow-up. All clinical diagnoses were blind to PIB and FDG-PET results.

Criteria for PPA variants were adapted from previous publications^{2, 12, 13, 16} and recently reviewed at a PPA workshop attended by senior investigators in the field. For each syndrome, patients were required to show the following features: *PNFA*: (i) motor speech deficits; (ii) agrammatism in language production; (iii) deficit in comprehension of complex sentences; (iv) spared single-word comprehension and object knowledge. *SD*: (i) fluent and grammatically correct language output; (ii) semantic memory deficit; (iii) confrontation naming deficit; (iv) surface dyslexia. *LPA*: (i) word retrieval deficits in spontaneous speech and confrontation naming; (ii) impaired repetition of sentences; (iii) errors in spontaneous speech and naming (e.g. phonological errors); (iv) sparing of word and object knowledge and motor speech.

Eligible patients were recruited consecutively between October 2005 and July 2007. The final cohort consisted of four patients with LPA, six with PNFA and five with SD (Table 1). One patient in each group was diagnosed based on a single evaluation and the remainder had longitudinal data. PET data for three patients (two with SD and one with PNFA) have been previously reported in a study of PIB-PET in AD and FTLD.³³ An additional two subjects with SD reported in our previous series (including one with elevated PIB uptake) were not included in the present study since they did not meet strict PPA criteria due to early impairment in non-language cognitive domains. One of the patients in this study (with a diagnosis of SD) was included in a previous report describing the language and MRI features of the three PPA variants.¹²

Records of neurological examinations were retrospectively reviewed (by GDR) to assess the presence of limb apraxia, parkinsonism (rigidity, bradykinesia, rest tremor, or postural instability) or upper-motor-neuron signs (spastic speech or tone, hyper-reflexia, or Babinski signs) during each patient's initial and most recent assessment (Table 1).

Structural Imaging

All patients underwent high resolution MRI scans on a 1.5-T Magnetom VISION system (Siemens Inc., Iselin, NJ) at the San Francisco Veterans Administration Medical Center according to a previously published protocol.¹⁹ In patients with multiple MRIs, the MRI closest to the date of the PET scan was used for analysis.

PET Radiochemistry and Acquisition

[N-methyl-¹¹C]-2-(4'-methylaminophenyl)-6-hydroxybenzothiazole ([¹¹C]PIB) was synthesized at the Lawrence Berkeley National Laboratory's Biomedical Isotope Facility using a previously published protocol.³³ ¹⁸F-fluorodeoxyglucose ([¹⁸F]FDG) was purchased from a commercial vendor (Eastern Isotopes, Sterling, VA). PET scans were performed at Lawrence Berkeley National Laboratory using a Siemens ECAT EXACT HR PET scanner in 3D acquisition mode. 12–15 mCi of [¹¹C]PIB was injected as a bolus into an antecubital vein. Dynamic acquisition frames were obtained over 90 minutes as previously described.³³ Fourteen of 15 patients also underwent [¹⁸F]FDG imaging. Patients were injected with 8–10 mCi of [¹⁸F]FDG and 30 minutes of emission data were collected at $t = 30 - 60$ min following tracer injection with patients quietly resting with eyes and ears unoccluded.³³ FDG scanning was started at a minimum of two hours following [¹¹C]PIB injection (six Carbon-11 half-lives). Ten minute transmission scans for attenuation correction were obtained either immediately before or after each [¹¹C]PIB and [¹⁸F]FDG scan. PET data were reconstructed using an ordered subset expectation maximization algorithm with weighted attenuation. Images were smoothed with a 4mm Gaussian kernel with scatter correction. All images were evaluated prior to analysis for patient motion and adequacy of statistical counts.

PET Processing and Analysis

All image processing and analysis was performed in SPM2 (<http://www.fil.ion.ucl.ac.uk/spm>). Reference regions in the pons (for FDG) and whole cerebellum (for PIB) were created in Montreal Neurological Institute (MNI) space⁴³ and then warped to each subject's native space using a previously described "reverse normalization" procedure.³³ Normalization errors (e.g. inclusion of CSF spaces within the warped ROIs) were manually corrected after superimposing the "reverse normalized" regions on the patient's native-space T1-weighted MRI (FSL software, <http://www.fmrib.ox.ac.uk/fsl>). PET-FDG frames were summed and normalized to mean activity in the pons for each subject.⁴⁴ For PIB, voxel-wise Distribution Volume Ratios (DVRs) were calculated using Logan graphical analysis,⁴⁵ with the cerebellum ROI time-activity curve used as a reference tissue input function.⁴⁶ Kinetic parameters ($t = 35 - 90$ min, $k_2 = 0.15 \text{ min}^{-1}$) were based on previously reported values.⁴⁶

In order to correct for the potential confounding effects of atrophy on PET data, we applied a two-compartmental partial volume correction to all PIB and FDG volumes. The correction procedure involves convolving a manually touched-up brain mask (composed of the gray and white matter segmented images from the subject's T1-weighted MRI) with the point spread function specific to the PET tomograph along all axes (previously empirically derived⁴⁷). This provides a means for calculating the percentage of brain tissue emitting tracer at each voxel. The PET count for each voxel is then adjusted based on the percentage of brain matter.⁴⁸ ⁴⁹ Following partial volume correction, PIB and FDG data were coregistered to the subject's T1-weighted MRI. To allow across-subjects comparisons, each subject's T1-weighted MRI

was normalized to MNI space using the SPM T1 template, and the derived normalization parameters were applied to the subject's coregistered PIB and FDG volumes.

One patient (with PNFA) requested to terminate the PIB scan at 80 min. PIB DVR values for this patient were calculated for $t = 35 - 80$ min. This patient did not undergo an FDG scan. In another patient (with LPA) it was not possible to create PIB DVR images due to severe motion artifact. Visual inspection (see below) for this subject was performed on Standardized Uptake Value images (cerebellar reference, $t = 30 - 50$ min)⁴⁶, but this patient was excluded from quantitative analyses of PIB uptake and lateralization because of the different image analysis method. Motion artifact was not a problem in analyzing this participant's FDG scan.

Visual Inspection

Voxel-wise PIB DVR images from all subjects were qualitatively assessed by two investigators (WJJ and AJF) blind to clinical diagnosis. Scans were visually read as positive or negative for cortical PIB. A positive scan was defined as a DVR image in which uptake was substantially greater in cortex and striatum than in white matter. Visual inspection based on these criteria has been previously validated as a reproducible and reliable estimate of elevated PIB uptake when compared to quantitative analysis.^{33, 50} Inter-rater agreement for visual reads was 100%, and we thus report a single set of interpretations below.

Region of Interest Definition and Analysis

A priori PPA regions of interest (ROIs) were defined based on peak voxels identified in a previous study comparing MRI gray matter atrophy patterns in the three PPA variants.¹² All ROIs were created in MNI space on the SPM T1 template. A left Frontal ROI was created by drawing 10mm spheres centered in left inferior frontal gyrus (MNI coordinates $x=-48, y=15, z=25$) and left precentral gyrus/sulcus ($x=-43, y=4, z=49$), peak voxels of atrophy detected in the PNFA versus controls comparison in the previous study.¹² A right Frontal ROI was created by drawing spheres centered at the analogous coordinates in the right hemisphere ($x=48, y=15, z=25$ and $x=43, y=4, z=49$ respectively). Similarly, left and right Anterior Temporal ROIs were created surrounding prior peak-atrophy coordinates in SD versus controls (anterior hippocampus and amygdala ($x=\pm 24, y=-6, z=-21$) and temporal pole ($x=\pm 31, y=-5, z=-39$)). Left and right Temporo-Parietal ROIs were created based on maximum atrophy coordinates previously found in LPA versus controls (inferior parietal lobule ($x=\pm 45, y=-54, z=49$) and posterior middle temporal gyrus/superior temporal sulcus ($x=\pm 68, y=-24, z=-3$)). PPA ROIs for a single subject (with PNFA) are shown in the Supplementary Figure. The Frontal, Anterior Temporal and Temporo-Parietal ROIs were combined to generate a Cumulative PPA ROI. Finally, the Automated Anatomic Labeling (AAL) Atlas⁵¹ was used to define ROIs in Hippocampus and in "Whole Cortex" (the latter by combining all cortical AAL regions into a single ROI for each hemisphere).

In order to exclude PET tracer counts from white matter and CSF, all template-based ROIs were masked by individual subjects' gray matter images using a two-step procedure.⁵² First, each subject's T1-weighted MRI (already normalized to MNI space) was segmented into gray matter, white matter and CSF (SPM2 defaults). Next, each ROI was multiplied by the individual subject's gray matter image. The resulting subject-specific "masked ROIs" were then used to extract mean regional values from each subject's PIB DVR and pons-normalized FDG images in MNI space.

Lateralization indices (LIs) were calculated to compare left- and right-sided tracer uptake in ROIs according to the following formula: $LI(ROI) = (Left(ROI) - Right(ROI)) / (Mean(Left \& Right ROIs))$. Thus, positive LIs represent increased tracer uptake in the left ROI compared to the right, while negative values represent preferential right-sided uptake.

AD and Control Comparison Groups

In order to compare PIB and FDG data in PPA to patients with clinical AD, we identified a comparison group of 10 AD patients with PIB-positive scans, matched to PPA patients for age (PPA 65.0 ± 7.9 , AD 64.7 ± 8.0) and dementia severity, as measured by the Mini-Mental State Exam (MMSE; PPA 21.1 ± 7.7 , AD 20.4 ± 7.9) and Clinical Dementia Rating (CDR; PPA 0.7 ± 0.5 , AD 0.9 ± 0.2). AD patients were recruited from a research cohort followed at the UCSF-MAC Alzheimer's Disease Research Center. The diagnosis of AD was made in a consensus clinical conference based on standard research criteria (NINCDS-ADRDA).⁵⁵ AD patients underwent identical clinical evaluations (aside from detailed language testing) and imaging protocols to those described for PPA.

Twelve cognitively normal volunteers with PIB-negative scans were selected as a control group (mean age 73.9 ± 6.1 , mean MMSE 29.4 ± 0.7). Controls were recruited from the community by advertisement. All were free of significant medical illnesses and were not taking medications deemed to affect cognition. Control subjects were judged to be cognitively normal following an evaluation that included a medical history, functional assessment, neurological examination and neuropsychological testing with a battery of tests similar to those performed by patients. Five AD patients and four controls were included in a previously-published series.³³

Statistical Analysis

Group differences in continuous variables were examined using Kruskal-Wallis one-way analysis of variance by ranks or one-way analysis of variance (ANOVA) (for comparisons involving three groups), and the Mann-Whitney U test or two-tailed independent sample t-tests (for comparisons involving two groups). Two-tailed one sample t-tests were used to test the hypothesis that LIs were significantly different than 0 (representing significant lateralization). Dichotomous variables were analyzed using Fisher's Exact test. Statistical analyses were implemented in SPSS 14.0 for Windows (SPSS Inc., Chicago, IL).

The study was approved by the University of California Berkeley, University of California San Francisco and Lawrence Berkeley National Laboratory institutional review boards for human research.

Results

Patient Characteristics

Patient characteristics are shown in Table 1. There were no significant group differences in age (although LPA patients tended to be younger) or disease duration at initial clinical evaluation or at the time of PET. Functional impairment (as measured by the CDR) was similar across groups, though patients with PNFA tended to be least impaired while patients with SD tended to be most impaired. One patient with LPA and one with SD carried the apolipoprotein E4 allele (both were E3/E4). Patients with LPA were more likely to be treated with acetylcholinesterase inhibitors. Motor system abnormalities were most common in PNFA, and upper-motor-neuron (UMN) signs were found exclusively in this group. In contrast, motor signs of any kind were rarely found in SD. With longitudinal follow-up, patients in the PNFA group developed limb apraxia, parkinsonism and UMN signs, patients with LPA developed limb apraxia, while SD patients remained free of motor system involvement.

Language and Neuropsychologic Testing

Results of language testing at first evaluation stratified by PPA subtype are presented in Table 2, and individual test results for all subjects are available online in the Supplementary Table. WAB fluency scores were surprisingly similar in the three PPA subtypes, perhaps because the PNFA patients included in this study had relatively mild disease. Motor speech abnormalities

were exclusively found in PNFA. SD patients had the greatest deficits in confrontation naming, category fluency and word and object knowledge, while LPA patients had the greatest difficulty with repetition. Syntactic comprehension was relatively spared in SD in comparison to single word comprehension. In PNFA, comprehension was impaired only for complex morphosyntactic structures (CYCLE 9), indicating a deficit in receptive grammar. LPA patients showed impaired sentence comprehension on both Sequential Commands and CYCLE (regardless of grammatical complexity), likely due to deficits in auditory working memory.²³

Illustrative non-language neuropsychological test scores at first evaluation are also shown in Table 2 (by subtype) and in the Supplementary Table (individual scores). Performance on many of these tests can be confounded by aphasia, so results must be interpreted with caution in PPA patients. Patients with PNFA tended to have higher MMSE scores than patients with LPA or SD. Patients with SD showed the greatest impairment in verbal memory (California Verbal Learning Test) while visual memory scores (modified Rey-Osterrieth figure recall) were similar across groups. Patients with LPA were relatively more impaired on executive function tests and calculations. Visuospatial function, as measured by copy of the modified Rey-Osterrieth figure, was spared in all patients. Patients with SD endorsed more depressive symptoms and had a greater degree of behavioral impairment, as measured by the Neuropsychiatric Inventory.⁵⁶

PIB-PET

All four LPA patients had PIB-positive scans by visual read, while only 1/6 PNFA patients and 1/5 SD patients were PIB-positive ($p < 0.02$). Qualitatively, the pattern of PIB binding in positive cases was similar to the pattern seen in AD,^{30, 57} with elevated tracer uptake throughout frontal, parietal and lateral temporal cortex and striatum (Fig 1). PIB uptake appeared relatively symmetric between left and right hemispheres, and between language and non-language regions. The uptake patterns in the PIB-positive PNFA and PIB-positive SD patients were qualitatively similar to the patterns seen in LPA and AD. The uptake pattern in PIB-negative PPA mirrored the pattern seen in most normal controls, with mild tracer uptake in white matter tracts and brainstem and no appreciable cortical binding (Fig 1).³⁰

On quantitative analysis, PPA patients whose PIB images were visually read as positive had significantly higher Whole Cortical DVRs (2.14 ± 0.19 , range 1.93 – 2.37) than PPA patients whose scans were read as negative (1.27 ± 0.11 , range 1.10 – 1.47, $p < 0.0005$), validating the reliability of the visual reads in estimating PIB uptake. Whole Cortical DVRs in PIB-positive PPA were similar to those seen in AD (2.01 ± 0.28 , $p = 0.55$) while PIB-negative PPA Whole Cortical DVRs were similar to controls (1.31 ± 0.03 , $p = 0.96$).

PIB DVR values and lateralization indices (LI) are shown in Table 3 and Fig 2A. When all PIB-positive PPA cases were combined, there was a non-significant trend for asymmetric PIB deposition in favor of the left hemisphere in PIB-positive PPA in Frontal ($LI = 0.04 \pm 0.04$, $p = 0.13$), Temporo-Parietal ($LI = 0.06 \pm 0.06$, $p = 0.09$) and Cumulative PPA (0.02 ± 0.02 , $p = 0.16$) ROIs. However, this trend was also seen in AD (Fig 2A), where significant left lateralization was found in Frontal ($p < 0.05$) and Anterior Temporal ($p < 0.005$) ROIs and a strong trend was seen in the Cumulative PPA region ($p = 0.06$). Overall, LIs in PIB-positive PPA and AD were significantly different only in the Anterior Temporal ROI, where left lateralization was seen in AD but not in PIB-positive PPA ($p < 0.005$).

FDG-PET

In contrast to the diffuse pattern of PIB uptake seen in all PIB-positive PPA cases, FDG scans were more focal and varied qualitatively based on PPA subtype (Fig 3). Patients with PNFA showed asymmetric left frontal hypometabolism, though this was sometimes subtle. SD

patients showed prominent anterior temporal hypometabolism, left greater than right, while patients with LPA showed the greatest metabolic lesions in the left parietal and posterolateral temporal lobes. Right temporoparietal cortex was spared in LPA, in contrast to typical AD in which there was bilateral, relatively symmetric temporoparietal hypometabolism (Fig 3). Patients with PIB-positive PNFA and SD showed FDG uptake patterns that were similar to their PIB-negative counterparts (Table 3).

Quantitative FDG analysis confirmed that the regions of greatest metabolic asymmetry closely matched the clinical syndromes (Table 3, Fig 2B). Patients with LPA had the greatest asymmetry (in favor of left hypometabolism) in the Temporo-Parietal ROI, patients with PNFA in the Frontal ROI and patients with SD in the Anterior Temporal ROI (Fig 2B). When grouped together, PPA patients had asymmetric left hypometabolism across Whole Cortex ($p<0.01$), Frontal ($p<0.01$), Anterior Temporal ($p<0.05$) and Cumulative PPA ($p<0.005$) ROIs, with a non-significant trend in the Temporo-Parietal ROI ($p=0.08$). Left hypometabolism was seen in AD across Whole Cortex ($p<0.05$) and the Temporo-Parietal ROI ($p<0.05$), whereas FDG uptake in AD in Frontal, Anterior Temporal and Cumulative PPA ROIs was symmetric (Fig 2B).

Two patients in the study were left-handed. One of these patients (with LPA) showed mild left-predominant PIB uptake (mean PPA LI = 0.03) and asymmetric left hypometabolism (Cumulative PPA LI = -0.15). The second had PIB-negative SD, with symmetric FDG uptake (Cumulative PPA LI = 0.00).

PIB-Positive PPA versus AD: Neuropsychological and Hippocampal PET Measures

To investigate cognitive, molecular and metabolic differences between PIB-positive PPA and AD, we performed post-hoc analyses comparing neuropsychometric test scores and hippocampal PET measures between the two groups. We expected that, consistent with the clinical diagnosis, PIB-positive PPA patients would show relative sparing of episodic memory (as well as other non-language cognitive functions), and that this would also be reflected in sparing of hippocampal glucose metabolism. In contrast, we anticipated that both PIB-positive PPA and AD patients would show low levels of hippocampal PIB uptake, as described in previous studies of PIB in AD,³⁰ and consistent with the relative paucity of fibrillar A β in hippocampus in AD pathologic studies.⁵⁸

As expected, PIB-positive PPA patients performed better than matched AD patients on tests of verbal and visual memory as well as on a visual construction task (Table 4). Comparison of language function was limited to confrontation naming and verbal fluency (since AD patients did not undergo comprehensive language testing), with non-significant trends for worse performance in PIB-positive PPA. Test performance in other cognitive domains was comparable between AD and PIB-positive PPA. The patients with PIB-positive PNFA and SD had similar language and cognitive profiles to PIB-negative patients with the same PPA subtype (Supplementary Table).

Mirroring the relative sparing of episodic memory in PIB-positive PPA, mean hippocampal glucose metabolism was significantly higher in PIB-positive PPA than in AD ($p<0.02$), and this difference was even more significant when the comparison was restricted to the LPA subtype (Table 3, $p<0.0005$). Hippocampal FDG uptake was significantly lower in AD than in controls ($p<0.0005$), but did not differ between PIB-positive PPA and controls ($p=0.74$) or between LPA and controls ($p=0.99$). In contrast, PIB uptake in hippocampus was similar in AD and PIB-positive PPA ($p=0.33$) and neither group differed significantly from controls (Table 3).

Discussion

In this study we applied PIB and FDG-PET to a clinically well characterized cohort of PPA patients in order to investigate *in vivo* the relationships between language phenotype, amyloid deposition and glucose metabolism in this disorder. The main findings were: 1) elevated PIB uptake was most frequently found in the logopenic variant of PPA (LPA, 4/4 patients), suggesting that this variant of progressive aphasia is often associated with underlying AD; 2) elevated PIB was uncommon in PNFA (1/6) and SD (1/5), suggesting that these PPA variants are not often associated with AD pathology; 3) patterns of glucose hypometabolism in PPA were focal and varied by clinical syndrome, while amyloid distribution in PIB-positive cases was diffuse and similar to AD.

LPA has only recently been introduced as a PPA variant, and patients with this clinical syndrome may still be misdiagnosed as having PNFA due to their decreased rate of speech.^{12, 23} However, the language features of LPA are distinguished from PNFA by the absence of apraxia of speech and dysarthria, the relative sparing of grammar in spontaneous speech, and the severe difficulty with repetition, especially of long sentences with unpredictable content.¹² These language features are most similar to vascular “conduction aphasia,” and may be caused by deficits in auditory working memory.^{12, 23, 59} Furthermore, the atrophy and glucose metabolism patterns in PNFA and LPA are distinct, with left temporoparietal lesions in LPA and left fronto-insular lesions in PNFA.¹² While FTLN-related pathology has most often been implicated in PNFA,^{5, 6} ten of fourteen patients retrospectively classified as LPA in recent clinicopathological series were found to have AD pathology on autopsy,^{9, 27} consistent with our finding that this language phenotype is predictive of underlying A β amyloidosis. Thus, accurately differentiating between LPA and PNFA has important implications for predicting underlying histopathology, and recognizing LPA as a unique variant of PPA may help identify PPA patients who are potential candidates for emerging anti-A β therapies.

We also found evidence of elevated PIB in one of six patients classified as PNFA and one of five subjects classified as SD. A retrospective review of these patients’ clinical data did not reveal atypical features (Supplementary Table). Furthermore, their FDG uptake patterns conformed to their clinical syndromes, and did not show the temporoparietal hypometabolism found in LPA or AD (Table 3). While PIB appears to be highly specific for A β ,^{30, 60} elevated PIB on PET does not exclude the presence of non-A β co-pathology. It is therefore possible that in addition to fibrillar A β , the PIB-positive PNFA and SD patients have co-morbid FTLN as the main pathology driving their aphasia syndrome, while A β pathology in these patients may be “clinically silent” or “age-related” (in the form of amyloid plaques, cerebral amyloid angiopathy, or both).^{31, 61} Alternatively, these patients may truly have AD pathology presenting with a PNFA or SD clinical and anatomic phenotype, as described in previous series.^{9, 62} Though we did not find PIB-negative cases of LPA in this study, it is likely that this syndrome can also be caused by FTLN-spectrum pathologies that asymmetrically affect temporoparietal cortex. As in all neurodegenerative diseases, deducing histopathology based on clinical phenotype in PPA relies on probabilistic relationships between clinical syndromes, anatomic patterns and underlying pathology. These relationships hold true at a group level, but are not always predictive at an individual level. Ultimately, biological markers such as PIB-PET may be needed to guide disease-specific treatment in individual patients presenting with PPA. Given the specificity of PIB for fibrillar A β ^{60, 63} and the strong correlations between *in vivo* PIB-PET signal and *in vitro* measures of A β found on autopsy,^{31, 32} PIB-PET may be a useful clinical tool for excluding AD pathology in patients presenting with any of the PPA variants.

Clarifying the relationships between the distribution of amyloid plaques, clinical symptoms and neuronal dysfunction is of utmost importance given the effort to develop treatments targeting A β plaques in AD.¹⁰ The ability to image A β pathology *in vivo* with PIB in patients with “focal” neurodegeneration such as PPA provides a unique opportunity to study these relationships and to compare them to the those found in AD. The pathology literature has been equivocal in this regard, with some investigators reporting a disproportionately high burden of plaques and tangles in left temporal and inferior parietal cortex in AD presenting as PPA,^{5, 64, 65} and others reporting a diffuse, “typical” pattern of AD pathology.^{6, 64} In a single case, Ng and colleagues found a higher burden of left hemisphere amyloid in a PIB-positive patient with PPA compared to patients with typical AD.⁶⁶ In contrast, we found that amyloid deposition in PPA was diffuse, involved language and non-language areas alike, and was qualitatively indistinguishable from the pattern seen in matched AD patients (Fig 1). Because most of our patients were imaged 5–6 years after the onset of their symptoms, we cannot exclude the possibility that amyloid deposition was more focal earlier in their disease course. However, at the time of imaging all patients with PIB-positive PPA in our study had a language-predominant syndrome in spite of the diffuse distribution of amyloid.

In contrast to the global pattern of PIB binding, FDG patterns in PPA were distinct and closely followed the clinical syndromes (Figs 2B, 3). In comparison to AD, hippocampal glucose metabolism was spared in PIB-positive PPA (Table 3), mirroring the clinical sparing of episodic memory (Table 4). FDG uptake in language-related areas was more asymmetric (in favor of left hemisphere hypometabolism) in PPA than in AD (Fig 2B), and the region of greatest hypometabolism in each PPA subtype closely followed the language phenotype, regardless of PIB-positivity (Fig 2B, Table 3).

The dissociation between PIB uptake and glucose metabolism found in our study is consistent with previous post-mortem and PIB studies in AD that have not found strong correlations between A β plaque distribution and clinical presentation, plaque load and disease severity, or plaque load and glucose metabolism in many brain regions (most notably frontal cortex and striatum).^{62, 67–72} There are many potential explanations for why patients with essentially identical A β plaque distribution patterns can have such discrepant clinical presentations and patterns of glucose metabolism. Patients may have discrete patterns of neurofibrillary tangles or soluble A β species (neither of which are imaged with PIB) that more closely match their clinical symptoms and metabolic patterns. Indeed, Mesulam and colleagues reported increased left hemisphere tangle pathology in AD presenting as PPA, while A β pathology was symmetric between hemispheres.²⁷ Alternatively, the incongruity between amyloid deposition and clinical phenotype may be caused by differential vulnerability of specific neural networks to a similar burden of A β pathology in different patients. While in most patients the hippocampal-medial temporal-posterior cingulate network may be most vulnerable to A β pathology,⁷³ resulting in the classical amnesic presentation of AD, in selected patients the language network may be most vulnerable, resulting in the clinical presentation of PPA. Differential vulnerability may be due to a combination of genetic, developmental and environmental factors that lead to decreased reserve or increased susceptibility to the neurotoxicity of A β . Further studies are needed to better elucidate the biological mechanisms of atypical presentations of AD.

Our study has a number of limitations. Histopathological confirmation is not available in any of our subjects (PPA or AD). While preliminary studies suggest strong correlations between *in vivo* PIB-PET signal and *in vitro* measures of A β found on autopsy,^{31, 32} further work is needed to validate the accuracy of PIB-PET in predicting underlying AD. As discussed above, we cannot exclude FTLD co-pathology in patients found to be PIB-positive, although the relatively young ages of our patients, particularly in the LPA group (Table 1), decreases the probability of “age-related” amyloid to some degree. The relatively small number of patients studied in each PPA subgroup limits our precision in estimating the prevalence of A β

amyloidosis in each variant, and limits our power to detect subtle differences in PIB and FDG uptake between PPA variants and between PPA and AD. Furthermore, the PIB data for one LPA patient was excluded from quantitative analyses for technical reasons, and the significance of tracer lateralization in another LPA patient who is left-handed is difficult to interpret due to the ambiguity of hemisphere dominance. Despite these limitations, our study demonstrates that PIB-PET is a promising diagnostic tool for excluding A β amyloidosis in PPA, and a useful research tool for studying the relationships between A β amyloid, clinical presentation, and neuronal structure and function.

In summary, using PIB-PET we have demonstrated an association between the logopenic variant of PPA and A β amyloidosis. Furthermore, we found that language phenotype in PPA is closely related to metabolic changes that are focal and anatomically distinct between PPA subtypes, but not to amyloid deposition patterns that are diffuse and similar to AD. Combining PIB-PET with careful clinical characterization and structural and functional imaging may improve *in vivo* predictions of underlying pathology in PPA, and help elucidate the relationships between amyloid deposition, clinical presentation and functional and structural changes in focal cortical presentations of AD. Further studies with larger numbers of patients followed to autopsy are needed to confirm our findings.

Supplementary Material

Refer to Web version on PubMed Central for supplementary material.

Acknowledgements

The authors would like to thank Dr. Suzanne Baker and Cindee Madison for technical support, and Victoria Beckman, Lovingly Quitania, Linda Isaac, Jung Jang and Matthew Growdon for administrative support. Funded by the John Douglas French Alzheimer's Foundation, Alzheimer's Association NIRG-07-59422, NINDS R01-NS050915, NIA AG027859 and P01-AG1972403, State of California DHS 04-33516, ADRC P50-AG023501.

References

1. Mesulam MM. Slowly progressive aphasia without generalized dementia. *Annals of Neurology* 1982;11:592–598. [PubMed: 7114808]
2. Mesulam MM. Primary progressive aphasia. *Ann Neurol* 2001;49:425–432. [PubMed: 11310619]
3. Sonty SP, Mesulam MM, Thompson CK, et al. Primary progressive aphasia: PPA and the language network. *Ann Neurol* 2003;53:35–49. [PubMed: 12509846]
4. Kertesz A, McMonagle P, Blair M, et al. The evolution and pathology of frontotemporal dementia. *Brain* 2005;128:1996–2005. [PubMed: 16033782]
5. Knibb JA, Xuereb JH, Patterson K, Hodges JR. Clinical and pathological characterization of progressive aphasia. *Ann Neurol* 2006;59:156–165. [PubMed: 16374817]
6. Forman MS, Farmer J, Johnson JK, et al. Frontotemporal dementia: clinicopathological correlations. *Ann Neurol* 2006;59:952–962. [PubMed: 16718704]
7. Josephs KA, Petersen RC, Knopman DS, et al. Clinicopathologic analysis of frontotemporal and corticobasal degenerations and PSP. *Neurology* 2006;66:41–48. [PubMed: 16401843]
8. Mesulam MM, Grossman M, Hillis A, et al. The core and halo of primary progressive aphasia and semantic dementia. *Ann Neurol* 2003;54 (Suppl 5):S11–14. [PubMed: 12833362]
9. Alladi S, Xuereb J, Bak T, et al. Focal cortical presentations of Alzheimer's disease. *Brain* 2007;130:2636–2645. [PubMed: 17898010]
10. Roberson ED, Mucke L. 100 years and counting: prospects for defeating Alzheimer's disease. *Science* 2006;314:781–784. [PubMed: 17082448]
11. Rosenberg RN. Translational research on the way to effective therapy for Alzheimer disease. *Arch Gen Psychiatry* 2005;62:1186–1192. [PubMed: 16275806]

12. Gorno-Tempini ML, Dronkers NF, Rankin KP, et al. Cognition and anatomy in three variants of primary progressive aphasia. *Ann Neurol* 2004;55:335–346. [PubMed: 14991811]
13. Neary D, Snowden JS, Gustafson L, et al. Frontotemporal lobar degeneration: a consensus on clinical diagnostic criteria. *Neurology* 1998;51:1546–1554. [PubMed: 9855500]
14. Hodges JR, Patterson K. Nonfluent progressive aphasia and semantic dementia: a comparative neuropsychological study. *Journal of the International Neuropsychological Society* 1996;2:511–524. [PubMed: 9375155]
15. Hillis AE, Tuffiash E, Caramazza A. Modality-specific deterioration in naming verbs in nonfluent primary progressive aphasia. *J Cogn Neurosci* 2002;14:1099–1108. [PubMed: 12419132]
16. Hodges JR, Patterson K, Oxbury S, Funnell E. Semantic dementia. Progressive fluent aphasia with temporal lobe atrophy. *Brain* 1992;115 (Pt 6):1783–1806. [PubMed: 1486461]
17. Nestor PJ, Graham NL, Fryer TD, et al. Progressive non-fluent aphasia is associated with hypometabolism centred on the left anterior insula. *Brain* 2003;126:2406–2418. [PubMed: 12902311]
18. Drzezga A, Grimmer T, Henriksen G, et al. Imaging of amyloid plaques and cerebral glucose metabolism in semantic dementia and Alzheimer's disease. *Neuroimage* 2008;39:619–633. [PubMed: 17962045]
19. Rosen HJ, Gorno-Tempini ML, Goldman WP, et al. Patterns of brain atrophy in frontotemporal dementia and semantic dementia. *Neurology* 2002;58:198–208. [PubMed: 11805245]
20. Hodges JR, Davies RR, Xuereb JH, et al. Clinicopathological correlates in frontotemporal dementia. *Ann Neurol* 2004;56:399–406. [PubMed: 15349867]
21. Neumann M, Sampathu DM, Kwong LK, et al. Ubiquitinated TDP-43 in frontotemporal lobar degeneration and amyotrophic lateral sclerosis. *Science* 2006;314:130–133. [PubMed: 17023659]
22. Davies RR, Hodges JR, Kril JJ, et al. The pathological basis of semantic dementia. *Brain* 2005;128:1984–1995. [PubMed: 16000337]
23. Gorno-Tempini ML, Brambati SM, Ginex V, et al. The logopenic/phonological variant of primary progressive aphasia. *Neurology*. in press
24. Kertesz A, Munoz DG. Primary progressive aphasia and Pick complex. *J Neurol Sci* 2003;206:97–107. [PubMed: 12480092]
25. Weintraub S, Rubin NP, Mesulam M-M. Primary progressive aphasia: longitudinal course, neuropsychological profile, and language features. *Arch Neurol* 1990;47:1329–1335. [PubMed: 2252450]
26. Karas GB, Burton EJ, Rombouts SA, et al. A comprehensive study of gray matter loss in patients with Alzheimer's disease using optimized voxel-based morphometry. *Neuroimage* 2003;18:895–907. [PubMed: 12725765]
27. Mesulam M, Wicklund A, Johnson N, et al. Alzheimer and frontotemporal pathology in subsets of primary progressive aphasia. *Ann Neurol*. 2008
28. Josephs KA, Whitwell JL, Duffy JR, et al. Progressive aphasia secondary to Alzheimer disease vs FTLN pathology. *Neurology* 2008;70:25–34. [PubMed: 18166704]
29. Nestor PJ, Balan K, Cheow HK, et al. Nuclear imaging can predict pathologic diagnosis in progressive nonfluent aphasia. *Neurology* 2007;68:238–239. [PubMed: 17224582]
30. Klunk WE, Engler H, Nordberg A, et al. Imaging brain amyloid in Alzheimer's disease with Pittsburgh Compound-B. *Ann Neurol* 2004;55:306–319. [PubMed: 14991808]
31. Bacskai BJ, Frosch MP, Freeman SH, et al. Molecular imaging with Pittsburgh Compound B confirmed at autopsy: a case report. *Arch Neurol* 2007;64:431–434. [PubMed: 17353389]
32. Ikonomic MD, Klunk WE, Abrahamson EE, et al. Post-mortem correlates of in vivo PiB-PET amyloid imaging in a typical case of Alzheimer's disease. *Brain*. 2008
33. Rabinovici GD, Furst AJ, O'Neil JP, et al. 11C-PIB PET imaging in Alzheimer disease and frontotemporal lobar degeneration. *Neurology* 2007;68:1205–1212. [PubMed: 17420404]
34. Rowe CC, Ng S, Ackermann U, et al. Imaging beta-amyloid burden in aging and dementia. *Neurology* 2007;68:1718–1725. [PubMed: 17502554]

35. Kramer JH, Jurik J, Sha SJ, et al. Distinctive neuropsychological patterns in frontotemporal dementia, semantic dementia, and Alzheimer disease. *Cogn Behav Neurol* 2003;16:211–218. [PubMed: 14665820]
36. Kertesz, A. *Western Aphasia Battery*. London, Ontario: University of Western Ontario Press; 1980.
37. Goodglass, H.; Kaplan, E. *The assessment of aphasia and related disorders*. Vol. 2. Philadelphia: Lea & Febiger; 1983. p. 101
38. Kaplan, E.; Goodglass, H.; Weintraub, S. *Boston Naming Test*. Philadelphia: Lea and Febiger; 1983.
39. Curtiss, S.; Yamada, J. *Curtiss-Yamada Comprehensive Language Evaluation*. 1988. Unpublished Test
40. Howard, D.; Patterson, K. *Pyramids and Palm trees: a test of semantic access from pictures and words*. Bury St Edmunds, Suffolk: Thames Valley Publishing Company; 1992.
41. Wertz, RT.; LaPointe, LL.; Rosenbek, JC. *Apraxia of Speech: The Disorders and Its Management*. New York: Grune and Stratton; 1984. p. 318
42. Kay, J.; Lesser, R.; Coltheart, M. *Psycholinguistics assessments of language processing in aphasia*. Hove, East Sussex: Lawrence Erlbaum Associates; 1992.
43. Holmes CJ, Hoge R, Collins L, et al. Enhancement of MR images using registration for signal averaging. *J Comput Assist Tomogr* 1998;22:324–333. [PubMed: 9530404]
44. Minoshima S, Frey KA, Foster NL, Kuhl DE. Preserved pontine glucose metabolism in Alzheimer disease: a reference region for functional brain image (PET) analysis. *J Comput Assist Tomogr* 1995;19:541–547. [PubMed: 7622680]
45. Logan J, Fowler JS, Volkow ND, et al. Distribution volume ratios without blood sampling from graphical analysis of PET data. *J Cereb Blood Flow Metab* 1996;16:834–840. [PubMed: 8784228]
46. Price JC, Klunk WE, Lopresti BJ, et al. Kinetic modeling of amyloid binding in humans using PET imaging and Pittsburgh Compound-B. *J Cereb Blood Flow Metab* 2005;25:1528–1547. [PubMed: 15944649]
47. Klein GJ, Teng X, Jagust WJ, et al. A methodology for specifying PET VOIs using multi-modality techniques. *IEEE Trans Med Imag* 1997;16:405–415.
48. Meltzer CC, Leal JP, Mayberg HS, et al. Correction of PET data for partial volume effects in human cerebral cortex by MR imaging. *J Comput Assist Tomogr* 1990;14:561–570. [PubMed: 2370355]
49. Meltzer CC, Kinahan PE, Greer PJ, et al. Comparative evaluation of MR-based partial-volume correction schemes for PET. *Journal of Nuclear Medicine* 1999;40:2053–2065. [PubMed: 10616886]
50. Ng S, Villemagne VL, Berlangieri S, et al. Visual assessment versus quantitative assessment of ¹¹C-PIB PET and ¹⁸F-FDG PET for detection of Alzheimer's disease. *J Nucl Med* 2007;48:547–552. [PubMed: 17401090]
51. Tzourio-Mazoyer N, Landeau B, Papathanassiou D, et al. Automated anatomical labeling of activations in SPM using a macroscopic anatomical parcellation of the MNI MRI single-subject brain. *Neuroimage* 2002;15:273–289. [PubMed: 11771995]
52. Sun FT, Schriber RA, Greenia JM, et al. Automated template-based PET region of interest analyses in the aging brain. *Neuroimage* 2007;34:608–617. [PubMed: 17112749]
53. Folstein MF, Folstein SE, McHugh PR. "Mini-mental state". A practical method for grading the mental state of patients for the clinician. *J Psychiat Res* 1975;12:189–198. [PubMed: 1202204]
54. Morris JC. The Clinical Dementia Rating (CDR): current version and scoring rules. *Neurology* 1993;43:2412–2414. [PubMed: 8232972][see comments]
55. Mckhann G, Drachman DA, Folstein M, et al. Clinical diagnosis of Alzheimer's disease: Report of the NINCDS-ADRDA Work Group under the auspices of Department of Health and Human Services Task Force on Alzheimer's Disease. *Neurology* 1984;34:939–944. [PubMed: 6610841]
56. Cummings JL. The Neuropsychiatric Inventory: assessing psychopathology in dementia patients. *Neurology* 1997;48:S10–16. [PubMed: 9153155]
57. Kempainen NM, Aalto S, Wilson IA, et al. Voxel-based analysis of PET amyloid ligand [¹¹C]PIB uptake in Alzheimer disease. *Neurology* 2006;67:1575–1580. [PubMed: 16971697]
58. Arnold SE, Hyman BT, Flory J, et al. The topographical and neuroanatomical distribution of neurofibrillary tangles and neuritic plaques in the cerebral cortex of patients in Alzheimer's disease. *Cerebral Cortex* 1991;1:103–116. [PubMed: 1822725]

59. Hillis AE, Selnes OA, Gordon B. Primary progressive “conduction aphasia”: a cognitive analysis of two cases. *Brain and Language* 1999;69:478–481.
60. Fodero-Tavoletti MT, Smith DP, McLean CA, et al. In vitro characterization of Pittsburgh compound-B binding to Lewy bodies. *J Neurosci* 2007;27:10365–10371. [PubMed: 17898208]
61. Johnson KA, Gregas M, Becker JA, et al. Imaging of amyloid burden and distribution in cerebral amyloid angiopathy. *Ann Neurol* 2007;62:229–234. [PubMed: 17683091]
62. Johnson J, Head E, Kim R, et al. Clinical and pathological evidence for a frontal variant of Alzheimer disease. *Arch Neurol* 1999;56:1233–1239. [PubMed: 10520939]
63. Klunk WE, Wang Y, Huang GF, et al. The binding of 2-(4'-methylaminophenyl)benzothiazole to postmortem brain homogenates is dominated by the amyloid component. *J Neurosci* 2003;23:2086–2092. [PubMed: 12657667]
64. Galton CJ, Patterson K, Xuereb JH, Hodges JR. Atypical and typical presentations of Alzheimer’s disease: a clinical, neuropsychological, neuroimaging and pathological study of 13 cases. *Brain* 2000;123(Pt 3):484–498. [PubMed: 10686172]
65. Green J, Morris JC, Sandson J, et al. Progressive aphasia: a precursor of global dementia? *Neurology* 1990;40:423–429. [PubMed: 2314582]
66. Ng SY, Villemagne VL, Masters CL, Rowe CC. Evaluating atypical dementia syndromes using positron emission tomography with carbon 11 labeled Pittsburgh Compound B. *Arch Neurol* 2007;64:1140–1144. [PubMed: 17698704]
67. Wilcock GK, Esiri MM. Plaques, tangles and dementia. A quantitative study. *J Neurol Sci* 1982;56:343–356. [PubMed: 7175555]
68. Guillozet AL, Weintraub S, Mash DC, Mesulam MM. Neurofibrillary tangles, amyloid, and memory in aging and mild cognitive impairment. *Arch Neurol* 2003;60:729–736. [PubMed: 12756137]
69. Prohovnik I, Perl DP, Davis KL, et al. Dissociation of neuropathology from severity of dementia in late-onset Alzheimer disease. *Neurology* 2006;66:49–55. [PubMed: 16401845]
70. Engler H, Forsberg A, Almkvist O, et al. Two-year follow-up of amyloid deposition in patients with Alzheimer’s disease. *Brain*. 2006
71. Edison P, Archer HA, Hinz R, et al. Amyloid, hypometabolism, and cognition in Alzheimer disease. An [11C]PIB and [18F]FDG PET study. *Neurology*. 2006
72. Forsberg, A.; Engler, H.; Almkvist, O., et al. *Neurobiol Aging*. 2007. PET imaging of amyloid deposition in patients with mild cognitive impairment.
73. Buckner RL, Snyder AZ, Shannon BJ, et al. Molecular, structural, and functional characterization of Alzheimer’s disease: evidence for a relationship between default activity, amyloid, and memory. *J Neurosci* 2005;25:7709–7717. [PubMed: 16120771]

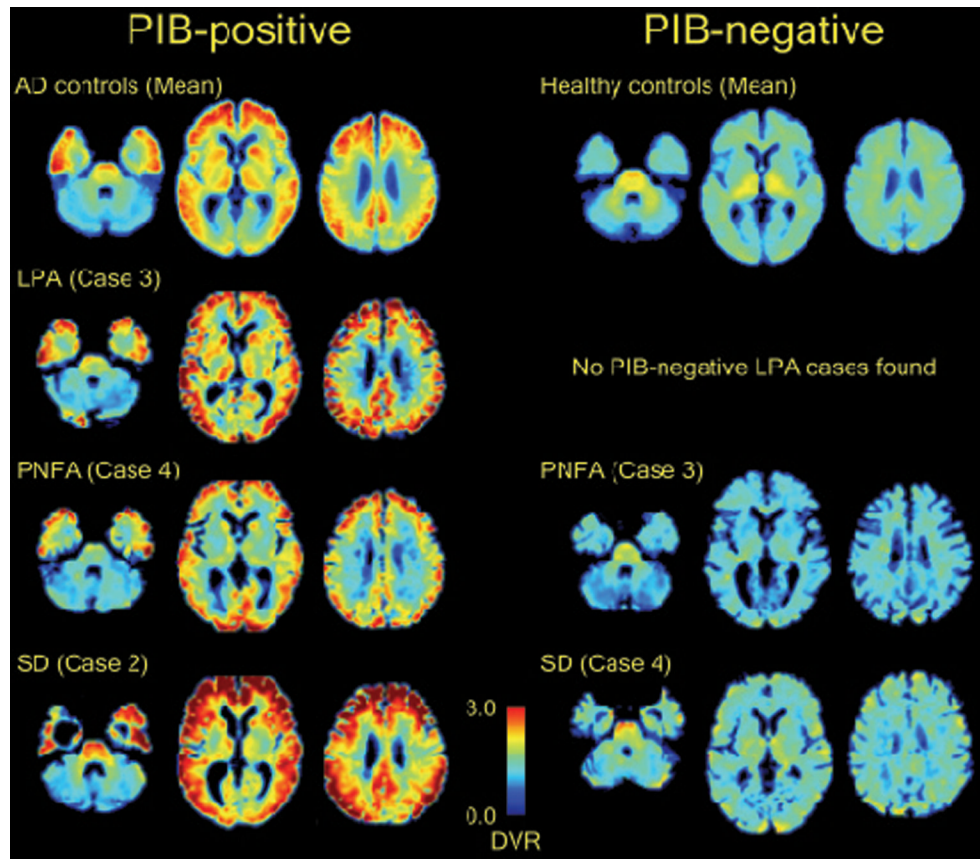


Fig 1. Distribution of PIB in PPA. Axial slices ($z = 9$, $z = 27$, $z = 41$) of normalized, atrophy-corrected PIB DVR images from single PIB-positive (left column) and PIB-negative (right column) PPA patients are presented. Identical slices from mean atrophy-corrected PIB DVR images from patients with AD ($N = 10$, top left) and normal controls ($N = 12$, top right) are shown for comparison. Images are in neurological orientation.

ROI Lateralization Indices

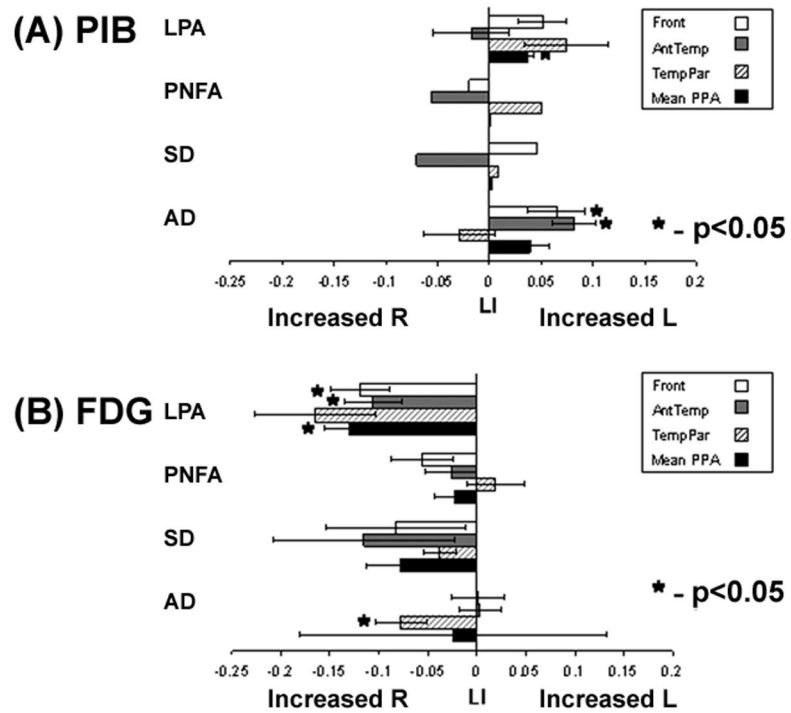


Fig 2. Mean lateralization indices (LI) for (A) PIB and (B) FDG. Bar graphs represent mean \pm standard error for each PPA subtype and for AD in frontal (Front), anterior temporal (AntTemp), temporoparietal (TempPar) and Cumulative PPA (Mean PPA) regions of interest. Asterisks mark values significantly different than 0 indicating lateralization ($p < 0.05$, one sample two-tailed t-test).

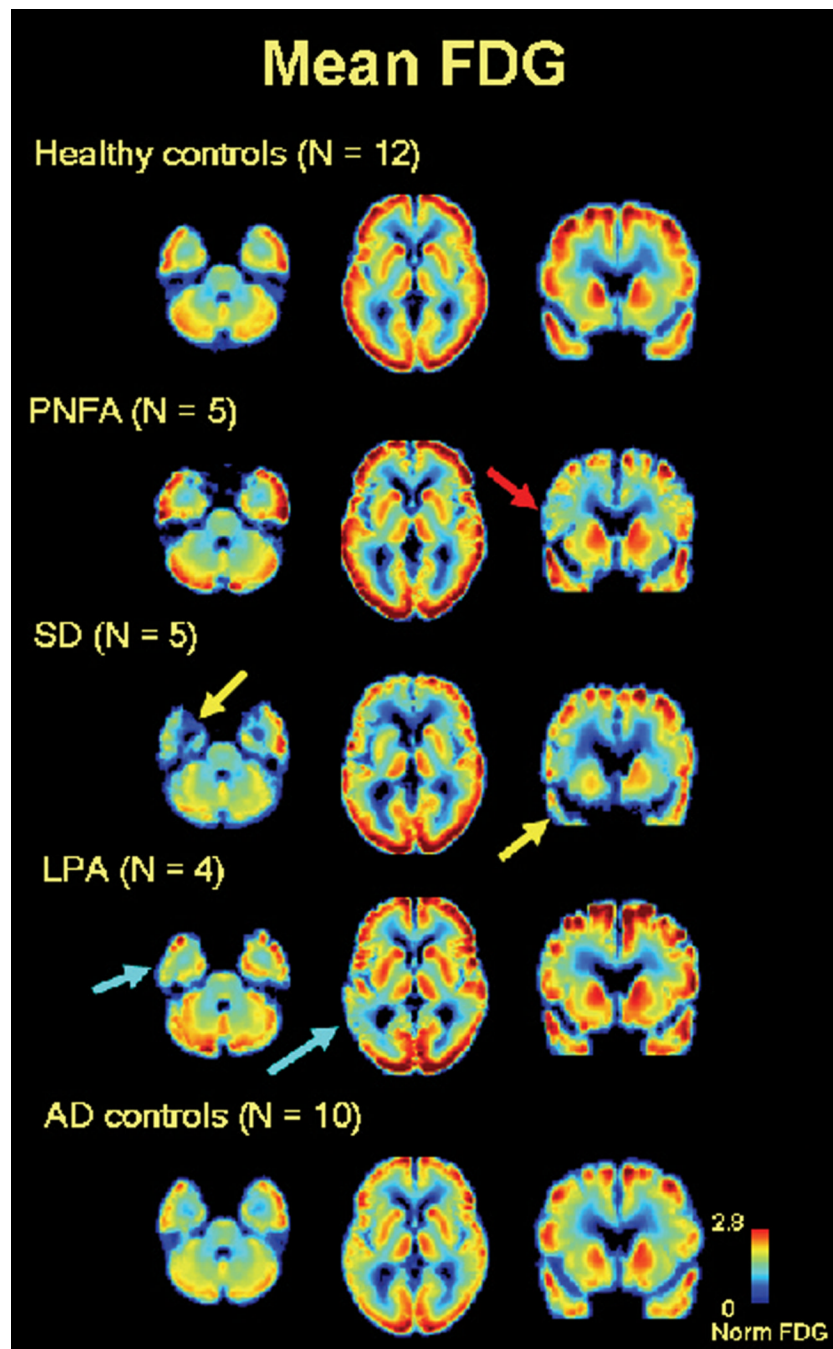


Fig 3. FDG patterns by clinical syndrome. Axial ($z = 9$, $z = 27$) and coronal ($y = 64$) slices of mean atrophy-corrected FDG images from (top to bottom) normal controls (N = 12), PNFA (N = 5), SD (N = 5), LPA (N = 4) and AD (N = 10). Images are in neurological orientation. PNFA is characterized by left frontal hypometabolism (red arrow), SD by left greater than right anterior temporal hypometabolism (yellow arrows), and LPA by asymmetric left temporoparietal hypometabolism (light blue arrows).

Table 1

Patient Characteristics

	LPA N=4	PNFA N=6	SD N=5	P
Age at PET (yrs)	60.1 (56.6 – 63.4)	68.1 (54.8 – 79.5)	62.2 (58.3 – 81.0)	0.24
Age at Onset (yrs)	54.0 (50.7 – 55.9)	63.5 (50.4 – 72.8)	56.8 (53.3 – 77.6)	0.19
Sex (M : F)	1 : 3	0 : 6	2 : 3	0.25
Hand (R : L)	3 : 1	6 : 0	4 : 1	0.45
Disease duration at PET (yrs)	6.1 (5.9 – 7.5)	6.2 (2.0 – 7.2)	5.4 (3.4 – 6.6)	0.45
Disease duration at first evaluation (yrs)	3.2 (3.0 – 7.4)	3.1 (1.6 – 6.3)	3.6 (1.9 – 5.8)	0.75
First evaluation to PET (yrs)	2.8 (0.1 – 3.1)	1.8 (0.1 – 4.1)	1.3 (0.3 – 3.5)	0.93
MMSE at PET	19.0 (12 – 23)	27.5 (4 – 28)	21.0 (8 – 26)	0.11
CDR at PET- Total	0.5 (0.5 – 1.0)	0.5 (0.0 – 1.0)	1.0 (0.5 – 2.0)	0.36
-SOB	4.0 (1 – 6)	1.8 (0 – 6)	5.0 (2 – 10)	0.29
Apo E4 pos/neg	1/4	0/6	1/5	0.45
Medications				
ChE-I	4/4	0/6	1/5	0.03
Memantine	3/4	3/6	4/5	0.53
SSRI/SNRI	1/4	4/6	3/5	0.41
Motor signs				
First visit				
Limb apraxia	2/4	2/6	0/5	0.22
Parkinsonism	2/4	3/6	1/5	0.54
UMN	0/4	3/6	0/5	0.06
Recent visit				
Limb apraxia	3/4	4/6	0/5	0.02
Parkinsonism	1/4	5/6	1/5	0.07
UMN	0/4	4/6	0/5	0.02

Values are presented as medians (range). LPA = logopenic aphasia; PNFA = progressive non-fluent aphasia; SD = semantic dementia; CDR = Clinical Dementia Rating; SOB = sum of boxes; Apo E4 = apolipoprotein E4; ChE-I = acetylcholinesterase inhibitor; SSRI = selective serotonin reuptake inhibitor; SNRI = serotonin norepinephrine reuptake inhibitor; UMN = upper motor neuron signs.

Table 2
Cognitive Testing at First Evaluation

	LPA N=4	PNFA N=6	SD N=5	P
MMSE (30)	22.0 (17 – 25)	27.0 (23 – 30)	21.0 (15 – 29)	0.052
Language				
WAB Fluency (10)	9.0 (5 – 9)	9.0 (2 – 9)	9.0 (8 – 10)	0.30
Motor Speech Evaluation				
Apraxia of Speech (0=none – 7=severe)	0.0 (0 – 0)	1.5 (0 – 6)	0.0 (0 – 0)	0.03
Dysarthria (0=none – 7=severe)	0.0 (0 – 0)	2.0 (0 – 4)	0.0 (0 – 0)	0.03
Boston Naming Test (15)	13.0 (11 – 14)	13.5 (6 – 15)	2.0 (2 – 3)	0.01
Verbal Fluency				
Animals/min	10.5 (8 – 16)	10.0 (0 – 22)	4.0 (1 – 7)	0.05
'D' words/min	7.0 (5 – 18)	4.0 (3 – 13)	6.0 (1 – 9)	0.31
Word and object knowledge				
WAB Auditory Word Recognition (60)	57.0 (52 – 60)	60.0 (59 – 60)	51.0 (36 – 59)	0.02
PPT Pictures (52)	51.0 (47 – 52)	49.0 (40 – 52)*	35.0 (31 – 48)	0.03
WAB Repetition (100)	75.0 (74 – 80)	97.0 (74 – 100)	90.5 (73 – 99)*	0.17
Syntactic Comprehension				
WAB Sequential Commands (80)	63.0 (37 – 68)	76.0 (63 – 80)	69.0 (66 – 80)*	0.10
CYCLE (2=simplest, 9=most complex)				
CYCLE 2, 3 (10)	10.0 (8 – 10)	10.0 (10 – 10)	10.0 (9 – 10)	0.46
CYCLE 4 (15)	14.5 (6 – 15)	15.0 (10 – 15)	15.0 (14 – 15)	0.56
CYCLE 5, 7 (10)	6.5 (3 – 9)	9.5 (4 – 10)	10.0 (5 – 10)	0.15
CYCLE 8 (10)	6.0 (4 – 9)	10.0 (5 – 10)	10.0 (9 – 10)	0.04
CYCLE 9 (10)	4.0 (2 – 7)	7.5 (3 – 10)	9.0 (6 – 10)	0.15
Memory				
CVLT-SF Total Learning (36)	22.0 (9 – 22)*	26.0 (14 – 29)*	9.0 (2 – 19)	0.054
CVLT-SF 10 minute Recall (9)	5.0 (0 – 5)*	8.0 (1 – 8)*	1.0 (0 – 5)	0.06
CVLT-SF Recognition (9)	9.0 (8 – 9)*	9.0 (8 – 9)*	7.0 (0 – 8)	0.02
Modified Rey Figure Recall (17)	6.5 (3 – 15)	6.5 (0 – 13)	7.0 (0 – 13)	0.83
Executive Function				
Modified Trails Time (120)	120.0 (73 – 120)	97.0 (21 – 120)	53.0 (36 – 120)	0.48
Modified Trails # of Correct Lines (14)	10.5 (0 – 14)	11.0 (3 – 14)	14.0 (3 – 14)	0.36
Calculations (5)	3.0 (1 – 5)	5.0 (2 – 5)	5.0 (0 – 5)	0.38
Modified Rey Figure Copy (17)	15.5 (13 – 17)	16.0 (14 – 17)	16.0 (12 – 17)	0.83
Mood & Personality				
Geriatric Depression Scale (30)	4.0 (2 – 12)	5.0 (2 – 28)	10.0 (6 – 20)	0.24
Neuropsychiatric Inventory Total	8.0 (2 – 23)	8.0 (0 – 24)*	16.0 (4 – 32)	0.61

* - One observation missing. Values are presented as medians (range). Highest possible test scores are shown in parentheses. LPA = logopenic aphasia; PNFA = progressive non-fluent aphasia; SD = semantic dementia; MMSE = Mini Mental State Exam; WAB = Western Aphasia Battery; PPT = pyramids and palm trees test; CYCLE = Curtiss-Yamada Comprehensive Language Evaluation; CVLT-SF = California Verbal Learning Test San Francisco.

Table 3

PET Tracer Uptake by Region of Interest

PIB DVR	LPA (N=3)*			PNFA (N=6)			SD (N=5)			AD (N=10)		CONT (N=12)	
	PIB-Pos (3)	PIB-Pos (1)	PIB-Neg (5)	PIB-Pos (1)	PIB-Neg (5)	PIB-Pos (1)	PIB-Pos (1)	PIB-Neg (4)	PIB-Pos (10)	PIB-Neg (12)	AD (N=10)	CONT (N=12)	
Whole Cortex	L	2.16 ± 0.08	1.90	1.31 ± 0.07	2.39	1.19 ± 0.09	2.04 ± 0.09	1.31 ± 0.03	2.04 ± 0.09	1.31 ± 0.03	2.04 ± 0.09	1.31 ± 0.03	
	R	2.10 ± 0.10	1.96	1.35 ± 0.09	2.34	1.20 ± 0.10	1.99 ± 0.09	1.30 ± 0.03	1.99 ± 0.09	1.30 ± 0.03	1.99 ± 0.09	1.30 ± 0.03	
	LI	0.03 ± 0.01	-0.03	-0.03 ± 0.05	0.02	0.00 ± 0.04	0.03 ± 0.04	0.01 ± 0.02	0.03 ± 0.04	0.01 ± 0.02	0.03 ± 0.04	0.01 ± 0.02	
PPA ROIs	L	2.31 ± 0.06	1.86	1.34 ± 0.09	2.42	1.23 ± 0.15	2.11 ± 0.26	1.39 ± 0.10	2.11 ± 0.26	1.39 ± 0.10	2.11 ± 0.26	1.39 ± 0.10	
	R	2.19 ± 0.06	1.89	1.40 ± 0.09	2.31	1.18 ± 0.17	1.99 ± 0.38	1.38 ± 0.11	1.99 ± 0.38	1.38 ± 0.11	1.99 ± 0.38	1.38 ± 0.11	
	LI	0.05 ± 0.02	-0.02	-0.05 ± 0.07	0.05	0.04 ± 0.13	0.07 ± 0.09^d	0.00 ± 0.06	0.07 ± 0.09^d	0.00 ± 0.06	0.07 ± 0.09^d	0.00 ± 0.06	
AntTemporal	L	1.59 ± 0.08	1.49	1.28 ± 0.12	1.33	0.94 ± 0.13	1.65 ± 0.16	1.29 ± 0.06	1.65 ± 0.16	1.29 ± 0.06	1.65 ± 0.16	1.29 ± 0.06	
	R	1.62 ± 0.05	1.57	1.33 ± 0.12	1.43	1.11 ± 0.05	1.53 ± 0.19	1.27 ± 0.06	1.53 ± 0.19	1.27 ± 0.06	1.53 ± 0.19	1.27 ± 0.06	
	LI	-0.02 ± 0.04	-0.06	-0.04 ± 0.04	-0.07	-0.17 ± 0.11	0.08 ± 0.07^d	0.02 ± 0.06	0.08 ± 0.07^d	0.02 ± 0.06	0.08 ± 0.07^d	0.02 ± 0.06	
TemporoParietal	L	2.57 ± 0.15	2.24	1.35 ± 0.10	2.52	1.25 ± 0.17	2.09 ± 0.57	1.36 ± 0.09	2.09 ± 0.57	1.36 ± 0.09	2.09 ± 0.57	1.36 ± 0.09	
	R	2.38 ± 0.06	2.12	1.37 ± 0.16	2.50	1.18 ± 0.12	2.11 ± 0.45	1.37 ± 0.09	2.11 ± 0.45	1.37 ± 0.09	2.11 ± 0.45	1.37 ± 0.09	
	LI	0.07 ± 0.04	0.05	-0.01 ± 0.10	0.01	0.05 ± 0.08	-0.03 ± 0.11	-0.01 ± 0.10	-0.03 ± 0.11	-0.01 ± 0.10	-0.03 ± 0.11	-0.01 ± 0.10	
Cumulative PPA	L	2.16 ± 0.12	1.86	1.33 ± 0.08	2.09	1.14 ± 0.12	1.95 ± 0.29	1.34 ± 0.05	1.95 ± 0.29	1.34 ± 0.05	1.95 ± 0.29	1.34 ± 0.05	
	R	2.06 ± 0.08	1.86	1.37 ± 0.10	2.08	1.16 ± 0.10	1.88 ± 0.31	1.34 ± 0.06	1.88 ± 0.31	1.34 ± 0.06	1.88 ± 0.31	1.34 ± 0.06	
	LI	0.04 ± 0.01^d	0.00	-0.03 ± 0.04	0.00	-0.03 ± 0.05	0.04 ± 0.06	0.00 ± 0.03	0.04 ± 0.06	0.00 ± 0.03	0.04 ± 0.06	0.00 ± 0.03	
Hippocampus	B	1.22 ± 0.06	1.12	1.16 ± 0.06	1.18	1.01 ± 0.06	1.27 ± 0.07	1.19 ± 0.06	1.27 ± 0.07	1.19 ± 0.06	1.27 ± 0.07	1.19 ± 0.06	
Norm FDG	LPA (N=4)	PIB-Pos (4)	PNFA (N=5)	PIB-Pos (1)	PIB-Neg (4)	SD (N=5)	PIB-Pos (1)	PIB-Neg (4)	AD (N=10)	CONT (N=12)	PIB-Pos (10)	PIB-Neg (12)	
	L	2.07 ± 0.29	2.05	2.12 ± 0.13	2.21	1.87 ± 0.16	1.81 ± 0.26	2.07 ± 0.14	1.81 ± 0.26	2.07 ± 0.14	1.81 ± 0.26	2.07 ± 0.14	
Whole Cortex	R	2.24 ± 0.27	2.04	2.18 ± 0.10	2.31	1.91 ± 0.08	1.86 ± 0.25	2.06 ± 0.13	1.86 ± 0.25	2.06 ± 0.13	1.86 ± 0.25	2.06 ± 0.13	
	LI	-0.08 ± 0.03^d	0.01	-0.03 ± 0.03	-0.04	-0.02 ± 0.07	-0.03 ± 0.03^d	0.00 ± 0.02	-0.03 ± 0.03^d	0.00 ± 0.02	-0.03 ± 0.03^d	0.00 ± 0.02	
	L	2.25 ± 0.48	2.18	2.26 ± 0.21	2.62	1.98 ± 0.30	2.09 ± 0.38	2.46 ± 0.21	2.09 ± 0.38	2.46 ± 0.21	2.09 ± 0.38	2.46 ± 0.21	
PPA ROIs	R	2.47 ± 0.53	2.32	2.39 ± 0.19	2.67	2.16 ± 0.10	2.08 ± 0.32	2.33 ± 0.18	2.08 ± 0.32	2.33 ± 0.18	2.08 ± 0.32	2.33 ± 0.18	
	LI	-0.12 ± 0.06^d	-0.06	-0.06 ± 0.08	-0.02	-0.10 ± 0.18	0.00 ± 0.09	0.06 ± 0.06	0.00 ± 0.09	0.06 ± 0.06	0.00 ± 0.09	0.06 ± 0.06	

PIB DVR	LPA (N=3) [*]			PNFA (N=6)			SD (N=5)			AD (N=10)		CONT (N=12)	
		PIB-Pos (3)	PIB-Neg (3)	PIB-Pos (1)	PIB-Neg (5)	PIB-Pos (1)	PIB-Pos (1)	PIB-Neg (4)	PIB-Pos (10)	PIB-Neg (12)			
AntTemporal	L	1.55 ± 0.13	1.47 ± 0.12	1.46	1.08	1.16 ± 0.30	1.34 ± 0.15	1.53 ± 0.10					
	R	1.66 ± 0.20	1.53 ± 0.14	1.39	1.30	1.25 ± 0.09	1.34 ± 0.17	1.55 ± 0.15					
	LI	-0.11 ± 0.06^d	-0.04 ± 0.05	0.04	-0.19	-0.10 ± 0.23	0.00 ± 0.07	-0.01 ± 0.08					
TemporoParietal	L	1.89 ± 0.44	2.48 ± 0.35	2.36	2.40	1.99 ± 0.19	1.70 ± 0.45	2.33 ± 0.18					
	R	2.17 ± 0.32	2.38 ± 0.23	2.46	2.42	2.07 ± 0.18	1.85 ± 0.49	2.39 ± 0.21					
	LI	-0.16 ± 0.12	0.03 ± 0.07	-0.04	-0.01	-0.05 ± 0.04	-0.08 ± 0.08^d	-0.02 ± 0.04					
Cumulative PPA	L	1.88 ± 0.28	2.07 ± 0.17	2.00	2.03	1.71 ± 0.10	1.71 ± 0.30	2.11 ± 0.13					
	R	2.10 ± 0.28	2.10 ± 0.14	2.06	2.13	1.83 ± 0.05	1.76 ± 0.30	2.09 ± 0.14					
	LI	-0.13 ± 0.05^d	-0.02 ± 0.06	-0.03	-0.05	-0.07 ± 0.07	-0.02 ± 0.05	0.01 ± 0.04					
Hippocampus	B	1.29 ± 0.11	1.23 ± 0.08	1.15	1.02	0.98 ± 0.03^b	1.06 ± 0.07^b	1.28 ± 0.06					

* - One study excluded due to motion artifact.

^a - Significantly different than 0 (p<0.05).

^b - Significantly lower than LPA, PNFA and controls (p<0.005). Values are means ± standard deviations. PIB DVR = PIB distribution volume ratio with cerebellar reference; Norm FDG = FDG uptake normalized to pons; LPA = logopenic aphasia; PNFA = progressive non-fluent aphasia; SD = semantic dementia; AD = Alzheimer's disease; CONT = controls; L = left; R = right; B = bilateral; LI = lateralization index; AntTemporal = anterior temporal.

Table 4
Cognitive Profiles in PIB-Positive PPA and AD

	PIB-Pos PPA N = 6	AD N=10	P
Age at PET	61.2 (56.6 – 70.7)	65.2 (52.5 – 78.3)	0.26
MMSE (30)	23.5 (17 – 29)	25.0 (10 – 28)	0.79
Language			
Boston Naming Test	11.5 (3 – 14)	13.0 (2 – 15)	0.37
Animals/min	7.0 (4 – 18)	10.5 (2 – 18)	0.18
'D' words/min	9.5 (5 – 16)	10.0 (2 – 22)	0.71
Memory			
CVLT-SF Total Learning (36)*	21.0 (9 – 22)*	18.5 (6 – 25)**	0.52
CVLT-SF 10 minute Recall (9)**	5.0 (0 – 7)*	0.0 (0 – 5)*	0.06
CVLT-SF Recognition (9)**	9.0 (8 – 9)*	8.0 (5 – 9)*	0.24
Modified Rey Figure Recall (17)	6.0 (3 – 15)	1.0 (0 – 5)	0.01
Executive Function			
Modified Trails Time (120)	97.0 (53 – 120)	120.0 (59 – 120)*	0.61
Modified Trails # of Correct Lines (14)	12.5 (0 – 14)	13.0 (2 – 14)*	0.69
Calculations (5)	3.5 (1 – 5)	4.0 (0 – 5)	0.96
Modified Rey Figure Copy (17)	16.5 (13 – 17)	14.0 (10 – 16)	0.03
Geriatric Depression Scale (30)	8.0 (0 – 23)	6.0 (2 – 24)	0.88

* - One observation missing.

** - Two observations missing. Values are presented as medians (range). Highest possible test scores are shown in parentheses. MMSE = Mini Mental State Exam; CVLT-SF = California Verbal Learning Test San Francisco.